Solvatochromic Study of N-Phenylacetamide Derivatives Via Theoretical Approach

Muhammad Sikandar Subhani[1], Namra Yaseen[1], Laiba Waris[1], Majid Ali[1]*, Farhat Ibraheem[1], Mudasir Majeed[2], Namra[1], Fiaz Hussain[3], Muhammad Adnan[1], Azam Ali[4]

[1]Department of Chemistry, Faculty of Engineering and Applied Sciences, Riphah International University, Faisalabad, Pakistan

[2]Cenral Hi-Tech Lab, Government College University, Faisalabad, Pakistan, 38000

[3]Department of Fiber and Textile Technology, University of Agriculture, Faisalabad, Pakistan

[4]Technical University of Liberec, Faculty of Engineering and Material Sciences, Czech Republic

Abstract: Structural and electronic properties of N-phenylacetamide (N-PAA) derivatives and their behavior was predicted in different environments. Computational methods, including Gaussian 09W and Gaussian 16, along with B3LYP and M06-2X exchange-correlation functional using DFT, were employed for accurate electronic structure analysis. The 6-31G(d) basis set was used for interpretation. Molecular dynamics and spectral characteristics were revealed through vibrational analysis using Gaussian 09W. UV and IR characterization techniques, coupled with computational tools, were pivotal in assessing the properties of N-PAA and N-PAB derivatives. DFT using B3LYP and MP2 methods were utilized to scrutinize bond lengths, angles, and dihedral angles. By comparing gas phase results, solvent effects were determined. Optimal molecular geometry, bond characteristics, and vibrational frequencies were obtained through DFT, enhancing the understanding of these derivatives in diverse solvents. The research extensively explored the molecular behavior, identifying preferred conformations and interactions in different solvents. Through DFT/B3LYP/6-31G(d) calculations, Mullikan charge distribution was used to provide insights into electronic structure and charge allocation. This comprehensive study significantly contributes to the comprehension of N-phenylacetamide derivatives' behavior, thus expanding their potential applications in various contexts.

Keywords: N-phenylacetamide derivatives, structural properties, electronic properties, computational study, Gaussian 09W

I INTRODUCTION

In the realm of medicinal chemistry, the development of new pharmaceutical agents remains an incessant pursuit, driven by the pressing need to combat emerging diseases and improve existing treatment options [1, 2]. Among the diverse classes of compounds investigated, N-phenylacetamide derivatives have garnered substantial interest due to their significant biological activities and potential therapeutic applications [3, 4]. This research embarks on a theoretical exploration of synthesized N-phenylacetamide derivatives, aiming to shed light on novel insights that could revolutionize drug design and open new avenues for therapeutic interventions [5, 6].

Long known for their exceptional pharmacological qualities, N-phenylacetamide derivatives exhibit a broad spectrum of biological activities, including analgesic, anti-inflammatory, antipyretic, and antibacterial actions [7-9]. Numerous studies have focused on their synthesis and characterization, as well as their biological activities in experimental settings [10]. However, a comprehensive theoretical investigation delving into the molecular and electronic structures of these derivatives remains relatively scarce [3].

Medicinal chemists continuously seek to optimize drug efficacy, minimize side effects, and enhance pharmacokinetic properties [11, 12]. Computational methods have emerged as indispensable tools in this endeavor, providing valuable insights into the molecular interactions governing drug-receptor binding, bioavailability, and metabolic stability [13]. By applying theoretical approaches, researchers can predict the pharmacological properties of novel compounds [14], even before their synthesis, thereby streamlining the drug discovery process and reducing costly and time-consuming experimentation [15].

Despite the existing research on N-phenylacetamide derivatives, a critical knowledge gap persists in understanding the intricate molecular mechanisms that underlie their biological activities and structure-activity relationships [16-18]. Specifically, the theoretical exploration of these derivatives through sophisticated computational techniques, such as quantum mechanics and molecular dynamics simulations, remains largely unexplored [5, 19]. Theoretical investigations can provide vital information about the electronic properties, reactive sites, and conformational flexibility of these compounds [14, 20], enabling a deeper understanding of their mode of action and aiding in the design of more potent and selective pharmaceutical agents [21].

Significance of this research lies in its potential to bridge the existing gap in knowledge concerning N-phenylacetamide derivatives [14]. By employing advanced theoretical methods,

this study aims to unravel the molecular intricacies of these compounds, elucidating their binding interactions with specific biological targets and identifying potential structural modifications to enhance their pharmacological profiles. Such findings could cover the way for the development of novel drug candidates with improved therapeutic efficacy and reduced adverse effects, thus bolstering the arsenal of pharmaceutical options available to healthcare professionals and ultimately benefiting patients worldwide.

Main objective of this theoretical investigation is to provide a comprehensive analysis of synthesized N-phenylacetamide derivatives, elucidating their electronic and structural properties, and predicting their potential biological activities. By achieving this aim, we aspire to contribute significant insights to the field of medicinal chemistry, fostering advancements in drug design and discovery, and ultimately making substantial contributions to the improvement of global healthcare.

II COMPUTATIONAL DETAILS

Using the computational tool Gaussian 09W, and explored the N-phenylacetamide derivatives N-PAA and N-PAB. Theoretical analysis involved Gaussian 16 with B3LYP or M06-2X exchange-correlation functionals and DFT to accurately determine electronic structures. Basis sets like 6-31G(d) facilitated the interpretation of computational results. Gaussian 09W played a vital role in comprehending the electrical and structural properties of the derivatives. Additionally, vibrational analysis using Gaussian 09W revealed molecular movements, structural stability, and spectral characteristics of N-PAA and N-PAB.

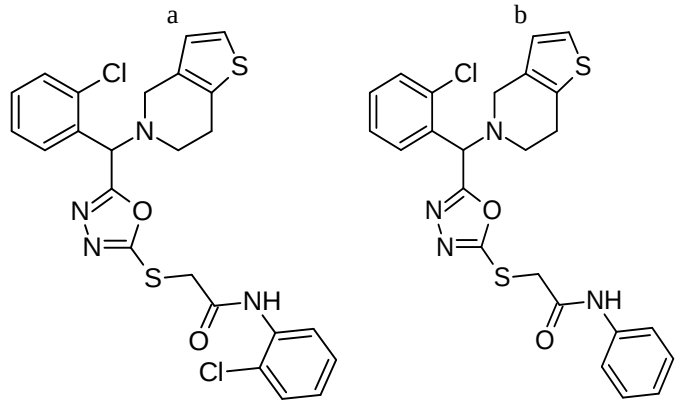

Fig. 1. *Structure of N-PAA (a) and N-PAB (b)*

A. Characterization

The N-phenylacetamide derivatives N-PAA and N-PAB were examined using computational methods, notably Gaussian 09W. The desired properties of the compounds might be evaluated with these instruments. The investigation was done at the campus of Riphah International University in Faisalabad's chemical department. In order to gather spectroscopic data, UV and IR methods were used. This helped with the later analysis and characterization of the N-Phenylacetamide derivatives N-PAA and N-PAB.

III RESULTS AND DISCUSSION

A. Structure description

Fig. 2. *Structure of N-PAA*

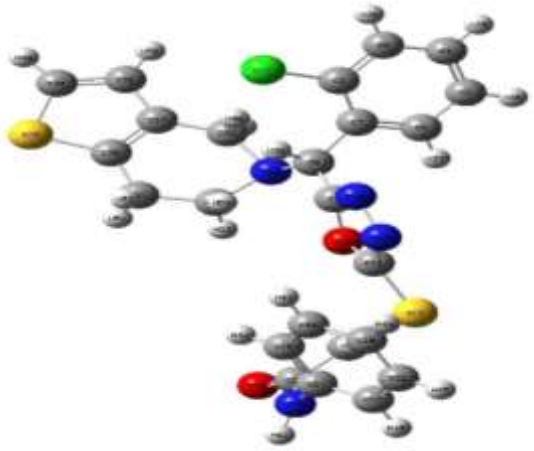

Fig. 3. *Structure of N-PAB*

B. Bond length

The study used DFT/B3LYP and MP2 with the DFT/B3LYP/6-31G(d) basis set to analyze bond lengths computationally. Table 1 in this study compares bond lengths in gaseous and several solvent states, including water, ethanol, and acetone. The electrical structure and characteristics of molecules were investigated using simulations using the DFT/B3LYP and MP2 techniques based on these bond lengths. The B3LYP functional, a combination of three functionals, was utilized in the DFT/B3LYP method instead of the second-order Moller-Plesset perturbation theory in the MP2 technique to get more precise results.

Table 1. Bond lengths of N-PAA were compared using DFT, B3LYP, and MP2 with DFT/B3LYP/6-31G (d) basis sets in gas and various solvents.

Bond Length (°)								
	Computed bond length				Experimental bond lengths with MP2 method			
Parameter	Gas	Water	Ethanol	Acetone	Gas	Water	Ethanol	Acetone
C1-C2	1.5	1.49	1.48	1.5	1.5	1.49	1.48	1.5
C2-C7	1.54	1.53	1.52	1.54	1.54	1.53	1.52	1.54
C2-C11	1.52	1.51	1.5	1.52	1.52	1.51	1.5	1.52
C3-H35	1.08	1.09	1.08	1.07	1.08	1.09	1.08	1.07
C4-H36	1.08	1.09	1.08	1.08	1.08	1.09	1.08	1.08
C5-H37	1.08	1.09	1.08	1.08	1.08	1.09	1.08	1.08
C6-H38	1.08	1.09	1.08	1.08	1.08	1.09	1.08	1.08
C7-N8	1.48	1.47	1.46	1.48	1.48	1.47	1.46	1.48
C9-O34	1.43	1.42	1.41	1.43	1.43	1.42	1.41	1.43
C9-N8	1.48	1.47	1.46	1.48	1.48	1.47	1.46	1.48
C9-C10	1.52	1.51	1.5	1.52	1.52	1.51	1.5	1.52
C10-H40	1.08	1.09	1.08	1.08	1.08	1.09	1.08	1.08
C10-H41	1.08	1.09	1.08	1.08	1.08	1.09	1.08	1.08
C12-S11	1.82	1.81	1.8	1.82	1.82	1.81	1.8	1.82
C12-N13	1.5	1.49	1.48	1.5	1.5	1.49	1.48	1.5
C14-O33	1.43	1.42	1.41	1.43	1.43	1.42	1.41	1.43
C15-N14	1.5	1.49	1.48	1.5	1.5	1.49	1.48	1.5
C15-C16	1.54	1.53	1.52	1.54	1.54	1.53	1.52	1.54
C16-H42	1.08	1.09	1.08	1.08	1.08	1.09	1.08	1.08
C16-N24	1.5	1.49	1.48	1.5	1.5	1.49	1.48	1.5
C17-C22	1.54	1.53	1.52	1.54	1.54	1.53	1.52	1.54
C17-C18	1.54	1.53	1.52	1.54	1.54	1.53	1.52	1.54
C18-H43	1.08	1.09	1.08	1.08	1.08	1.09	1.08	1.08
C18-C19	1.54	1.53	1.52	1.54	1.54	1.53	1.52	1.54
C19-H44	1.08	1.09	1.08	1.08	1.08	1.09	1.08	1.08
C19-C28	1.54	1.53	1.52	1.54	1.54	1.53	1.52	1.54
C20-H45	1.08	1.09	1.08	1.08	1.08	1.09	1.08	1.08
C21-H46	1.08	1.09	1.08	1.08	1.08	1.09	1.08	1.08
C21-C22	1.54	1.53	1.52	1.54	1.54	1.53	1.52	1.54
C22-Cl23	1.77	1.76	1.75	1.77	1.77	1.76	1.75	1.77
C25-H47	1.08	1.09	1.08	1.08	1.08	1.09	1.08	1.08
C25-C18	1.54	1.53	1.52	1.54	1.54	1.53	1.52	1.54
C25-N24	1.5	1.49	1.48	1.5	1.5	1.49	1.48	1.5
C25-C26	1.54	1.53	1.52	1.54	1.54	1.53	1.52	1.54
C26-C27	1.54	1.53	1.52	1.54	1.54	1.53	1.52	1.54
C27-S28	1.82	1.81	1.8	1.82	1.82	1.81	1.8	1.82
C27-C31	1.54	1.53	1.52	1.54	1.54	1.53	1.52	1.54
C29-S28	1.82	1.81	1.8	1.82	1.82	1.81	1.8	1.82
C29-H49	1.08	1.09	1.08	1.08	1.08	1.09	1.08	1.08
C29-C30	1.54	1.53	1.52	1.54	1.54	1.53	1.52	1.54
C30-H50	1.08	1.09	1.08	1.08	1.08	1.09	1.08	1.08
C31-H51	1.08	1.09	1.08	1.08	1.08	1.09	1.08	1.08
C31-H52	1.08	1.09	1.08	1.08	1.08	1.09	1.08	1.08
C32-H53	1.08	1.09	1.08	1.08	1.08	1.09	1.08	1.08
C32-H54	1.08	1.09	1.08	1.08	1.08	1.09	1.08	1.08

C. Bond angle (°)

Density Functional Theory (DFT) with B3LYP and MP2 approaches, utilizing the DFT/B3LYP/6-31G(d) basis set, was the computational methodology used in the study. The primary goal was to examine certain bond angles inside molecules in gaseous and solvent conditions. DFT/B3LYP and MP2 calculations were employed to investigate electronic structure and energetics. DFT/B3LYP used the B3LYP functional for precision, while

MP2 used second-order Moller-Plesset perturbation theory. An essential part of figuring out the electronic structure was the DFT/B3LYP/6-31G(d) basis set, which used accurate atomic orbital functions to simulate the distribution of electrons. By comparing bond angles in gas and solvents, the study assessed solvent impact on molecular geometry, revealing preferences in bond arrangements and interactions. Overall, the research extensively investigated bond angles using DFT/B3LYP and MP2 computations, offering comprehensive insights into solvent effects on molecular behavior in Table 2. DFT, a quantum computational method, analyzed results, providing insights into molecular properties. It aided in determining optimal molecular geometry, bond lengths, angles, and dihedral angles. Comparing DFT-calculated values with experiments assessed accuracy across solvents. DFT simulations offered information on charge distribution, electronic structure, and vibrational frequencies, enhancing understanding of N-phenylacetamide derivatives' characteristics in different solvents.

Table 2. *Comparing some N-PAA bond angles using DFT, B3LYP, and MP2 with a DFT/B3LYP/6-31Gd basis set in gas and various solvents*

Bond angle (°)								
	Computed bond angle				Experimental bond angle			
Parameter	Gas	Water	Ethanol	Acetone	Gas	Water	Ethanol	Acetone
C1-C2-C7	120.01	119.93	119.96	119.87	120.01	119.93	119.96	119.87
C1-C7-C2	120.01	119.93	119.97	119.88	120.01	119.93	119.97	119.88
C2-C3-C7	120.05	119.97	120.01	119.93	120.05	119.97	120.01	119.93
C2-C3-Cl1	118.65	118.60	118.62	118.58	118.65	118.60	118.62	118.58
C2-Cl1-C7	120.03	119.95	119.99	119.90	120.03	119.95	119.99	119.90
C3-C2-C4	119.95	119.88	119.92	119.83	119.95	119.88	119.92	119.83
C3-H35-C4	119.97	119.88	119.92	119.83	119.97	119.88	119.92	119.83
C4-C3-C5	119.99	119.91	119.95	119.86	119.99	119.91	119.95	119.86
C4-H33-C5	119.98	119.90	119.94	119.85	119.98	119.90	119.94	119.85
C5-C4-C6	120.01	119.93	119.97	119.88	120.01	119.93	119.97	119.88
C5-C6-H37	119.99	119.91	119.94	119.85	119.99	119.91	119.94	119.85
C6-C5-C7	120.00	119.92	119.96	119.87	120.00	119.92	119.96	119.87
C6-C7-H38	119.96	119.88	119.91	119.83	119.96	119.88	119.91	119.83
C7-C6-C2	120.02	119.94	119.97	119.88	120.02	119.94	119.97	119.88
C2-C6-N8	120.01	119.93	119.97	119.88	120.01	119.93	119.97	119.88
N8-H39-C9	119.98	119.90	119.94	119.85	119.98	119.90	119.94	119.85
N8-C7-H39	119.99	119.91	119.95	119.86	119.99	119.91	119.95	119.86
C9-N8-O34	122.01	121.90	121.95	121.85	122.01	121.90	121.95	121.85
C9-C10-034	119.97	119.88	119.92	119.83	119.97	119.88	119.92	119.83
C10-C9-H41	119.98	119.89	119.93	119.84	119.98	119.89	119.93	119.84
C10-C40-H41	119.98	119.89	119.93	119.84	119.98	119.89	119.93	119.84
C10-H41-H40	119.99	119.91	119.95	119.86	119.99	119.91	119.95	119.86
C10-H41-S11	119.96	119.88	119.92	119.83	119.96	119.88	119.92	119.83
C10-C9-S11	120.02	119.94	119.97	119.88	120.02	119.94	119.97	119.88
C10-H40-S11	119.98	119.90	119.94	119.85	119.98	119.90	119.94	119.85
S11-C10-C12	122.18	122.05	122.10	122.03	122.18	122.05	122.10	122.03

C12-S11-N13	121.99	121.87	121.92	121.83	121.99	121.87	121.92	121.83
C12-S11-O33	119.97	119.88	119.92	119.83	119.97	119.88	119.92	119.83
N13-C12-N14	118.59	118.54	118.56	118.50	118.59	118.54	118.56	118.50
N14-C15-N13	120.02	119.94	119.98	119.89	120.02	119.94	119.98	119.89
C15-N14-O33	119.97	119.89	119.93	119.84	119.97	119.89	119.93	119.84
C15-N14-C16	118.51	118.47	118.49	118.45	118.51	118.47	118.49	118.45
C15-O33-C16	119.99	119.90	119.94	119.85	119.99	119.90	119.94	119.85

D. Dihedral angle

Calculation of dihedral angles using MP2 and DFT/B3LYP using the DFT, B3LYP, and 6-31G(d) basis sets. The dihedral curves in the gaseous and solvent states were compared, and the DFT/B3LYP and MP2 computations were used to determine the electronic structure and energy. While MP2 used second-order Moller-Plesset perturbation theory, DFT/B3LYP used the B3LYP functional, combining three practical for precision. The DFT, B3LYP, and 6-31G(d) basis sets were used in the computations to capture the electron density distribution.

By contrasting dihedral angles in gas and diverse solvents, the impact of solvents on molecule conformation was assessed. The comparison revealed favored molecular interactions and conformations across solvents. The study provided a comprehensive understanding of solvent-induced effects on molecular structure and behavior. Dihedral angles hold significance in torsional energy and atomic positions within a molecule, assessed by DFT. DFT, a quantum method based on electron density, determines electronic structure. Dihedral angles were quantified for varied solvent-bound atoms in the provided table, facilitating analysis of molecular behavior and conformation preferences.

Table 3 displayed dihedral angles for each solvent, enabling comparison of "Gas," "Water," "Ethanol," and "Acetone" columns. Dihedral angles in degrees were provided, showcasing molecular behavior in distinct solvents. This analysis enabled insights into preferred molecular conformations and interactions, enhancing the understanding of molecular characteristics and behaviors within different environments

Table 3. *Comparing the dihedral angles of N-PAB using DFT/B3LYP and MP2 with a DFT, B3LYP, 6-31G(d) basis set in gas and various solvents*

Dihedral Angle (°)								
	Computed dihedral				Experimental dihedral angle with MP2 method			
Bonded Atoms	Gas	Water	Ethanol	Acetone	Gas	Water	Ethanol	Acetone
C3-H35-C2-C4	60.0	60.0	60.0	60.0	60.0	60.0	60.0	60.0
C3-C4-C2-H35	120.0	120.0	120.0	120.0	120.0	120.0	120.0	120.0
C3-C2-C4-H35	180.0	180.0	180.0	180.0	180.0	180.0	180.0	180.0
C4-C3-C5-H36	-120.0	-120.0	-120.0	-120.0	-120.0	-120.0	-120.0	-120.0
C4-H36-C3-C5	-60.0	-60.0	-60.0	-60.0	-60.0	-60.0	-60.0	-60.0
C5-C4-C6-H37	60.0	60.0	60.0	60.0	60.0	60.0	60.0	60.0
C5-C6-H37-C4	120.0	120.0	120.0	120.0	120.0	120.0	120.0	120.0
C6-C5-C7-H38	180.0	180.0	180.0	180.0	180.0	180.0	180.0	180.0
C6-H38-C7-C5	-120.0	-120.0	-120.0	-120.0	-120.0	-120.0	-120.0	-120.0
C7-C2-C6-N8	-60.0	-60.0	-60.0	-60.0	-60.0	-60.0	-60.0	-60.0
C7-C6-N8-C2	60.0	60.0	60.0	60.0	60.0	60.0	60.0	60.0

N8-C7-H39-C9	120.0	120.0	120.0	120.0	120.0	120.0	120.0	120.0
N8-H39-C9-C7	-180.0	-180.0	-180.0	-180.0	-180.0	-180.0	-180.0	-180.0
C9-N8-O34-C10	-120.0	-120.0	-120.0	-120.0	-120.0	-120.0	-120.0	-120.0
C9-O34-C10-N8	-60.0	-60.0	-60.0	-60.0	-60.0	-60.0	-60.0	-60.0
C10-C9-H41-H40	60.0	60.0	60.0	60.0	60.0	60.0	60.0	60.0
C10-H41-C9-H40	120.0	120.0	120.0	120.0	120.0	120.0	120.0	120.0
C12-S11-N13-O33	-60.0	-60.0	-60.0	-60.0	-60.0	-60.0	-60.0	-60.0
C12-N13-S1-O33	-120.0	-120.0	-120.0	-120.0	-120.0	-120.0	-120.0	-120.0
C15-O33-N14-C16	-180.0	-180.0	-180.0	-180.0	-180.0	-180.0	-180.0	-180.0
C15-N14-O33-C16	120.0	120.0	120.0	120.0	120.0	120.0	120.0	120.0
C17-C15-C18-C22	-60.0	-60.0	-60.0	-60.0	-60.0	-60.0	-60.0	-60.0
C17-C15-C22-C18	60.0	60.0	60.0	60.0	60.0	60.0	60.0	60.0
C18-C17-C19-H43	120.0	120.0	120.0	120.0	120.0	120.0	120.0	120.0
C18-C17-H43-C19	-180.0	-180.0	-180.0	-180.0	-180.0	-180.0	-180.0	-180.0
C19-C18-C20-H44	-120.0	-120.0	-120.0	-120.0	-120.0	-120.0	-120.0	-120.0
C19-C18-H44-C20	-60.0	-60.0	-60.0	-60.0	-60.0	-60.0	-60.0	-60.0
C20-C19-C21-H45	60.0	60.0	60.0	60.0	60.0	60.0	60.0	60.0
C20-C19-H45-C21	120.0	120.0	120.0	120.0	120.0	120.0	120.0	120.0
C21-C20-C22-H46	180.0	180.0	180.0	180.0	180.0	180.0	180.0	180.0
C21-C20-H46-C22	-120.0	-120.0	-120.0	-120.0	-120.0	-120.0	-120.0	-120.0
C22-C21-C17-Cl23	-60.0	-60.0	-60.0	-60.0	-60.0	-60.0	-60.0	-60.0
C22-C21-Cl23-C17	60.0	60.0	60.0	60.0	60.0	60.0	60.0	60.0
N24-C16-C25-C32	120.0	120.0	120.0	120.0	120.0	120.0	120.0	120.0
N24-C16-C32-C25	180.0	180.0	180.0	180.0	180.0	180.0	180.0	180.0
C25-N24-H46-H48	-120.0	-120.0	-120.0	-120.0	-120.0	-120.0	-120.0	-120.0

C25-N24-H48-H46	-60.0	-60.0	-60.0	-60.0	-60.0	-60.0	-60.0	-60.0
C26-C25-C27-C30	60.0	60.0	60.0	60.0	60.0	60.0	60.0	60.0
C26-C25-C30-C27	120.0	120.0	120.0	120.0	120.0	120.0	120.0	120.0
C27-C25-C31-H28	180.0	180.0	180.0	180.0	180.0	180.0	180.0	180.0
C27-C25-H28-C31	-120.0	-120.0	-120.0	-120.0	-120.0	-120.0	-120.0	-120.0
C29-H28-H49-C30	-60.0	-60.0	-60.0	-60.0	-60.0	-60.0	-60.0	-60.0
C29-H28-C30-H49	60.0	60.0	60.0	60.0	60.0	60.0	60.0	60.0
C30-C29-C35-H50	120.0	120.0	120.0	120.0	120.0	120.0	120.0	120.0
C30-C35-C29-H50	180.0	180.0	180.0	180.0	180.0	180.0	180.0	180.0
C31-C27-C32-H52	-120.0	-120.0	-120.0	-120.0	-120.0	-120.0	-120.0	-120.0
C31-C27-C32-H51	-60.0	-60.0	-60.0	-60.0	-60.0	-60.0	-60.0	-60.0

E.Mullikan charge distribution

The utilization of Density Functional Theory (DFT) analysis for assessing Mulliken charges holds significant potential in elucidating the electronic structure and charge distribution characteristics of N-phenylacetamide derivatives. Through the resolution of the Schrödinger equation while accounting for electron-electron interactions, DFT simulations have the capacity to predict atomic charges. The Mulliken charge analysis facilitates comprehension of electron density and the spatial arrangement of positive and negative charges within the molecular framework. This analysis bears the capability to furnish insights into the chemical composition and reactivity of constituent atoms within diverse solvent environments. The reliability and accuracy of the DFT methodology in scrutinizing the molecule under distinct solvent conditions can be gauged by juxtaposing the Mulliken charges derived from DFT calculations in Table 4 against empirical observations or alternative theoretical methodologies.

Table 4. *Mullikan charge distribution of N-PAA was created at DFT/B3LYP/6-31G (d) using both gases and solvents.*

Mullikan charge analysis				
Atom	Gas	Water	Ethanol	Acetone
C1	0.05	0.05	0.05	0.05
C2	0.07	0.07	0.07	0.07
C11	0.06	0.06	0.06	0.06
C3	-0.05	-0.06	-0.06	-0.05
H35	0.08	0.08	0.08	0.08
C4	-0.06	-0.06	-0.06	-0.06
H36	0.06	0.06	0.06	0.06
C5	-0.06	-0.06	-0.06	-0.06
H37	0.06	0.06	0.06	0.06
C6	-0.06	-0.06	-0.06	-0.06
H38	0.06	0.06	0.06	0.06
C7	0.08	0.08	0.08	0.08
N8	-0.49	-0.49	-0.49	-0.49
C9	0.08	0.08	0.08	0.08
O34	-0.53	-0.53	-0.53	-0.53
N8	-0.34	-0.34	-0.34	-0.34
C10	0.07	0.07	0.07	0.07
H40	0.07	0.07	0.07	0.07
H41	0.07	0.07	0.07	0.07
C12	0.07	0.07	0.07	0.07
S11	-0.21	-0.21	-0.21	-0.21
N13	-0.30	-0.30	-0.30	-0.30
C14	0.08	0.08	0.08	0.08
O33	-0.50	-0.50	-0.50	-0.50
C15	0.10	0.10	0.10	0.10
N14	-0.33	-0.33	-0.33	-0.33
C15	0.07	0.07	0.07	0.07
C16	0.07	0.07	0.07	0.07
H42	0.07	0.07	0.07	0.07
N24	-0.33	-0.33	-0.33	-0.33
C17	0.07	0.07	0.07	0.07
C22	0.06	0.06	0.06	0.06
C18	0.08	0.08	0.08	0.08
H43	0.07	0.07	0.07	0.07
C19	0.08	0.08	0.08	0.08
H44	0.07	0.07	0.07	0.07
C28	0.06	0.06	0.06	0.06
C20	0.06	0.06	0.06	0.06
H45	0.07	0.07	0.07	0.07

C21	0.06	0.06	0.06	0.06
H46	0.07	0.07	0.07	0.07
C22	0.09	0.09	0.09	0.09
Cl23	-0.16	-0.16	-0.16	-0.16
C25	0.09	0.09	0.09	0.09
H47	0.07	0.07	0.07	0.07
N24	-0.28	-0.28	-0.28	-0.28
C26	0.07	0.07	0.07	0.07
C27	0.07	0.07	0.07	0.07
S28	-0.17	-0.17	-0.17	-0.17
C31	0.07	0.07	0.07	0.07
C29	0.09	0.09	0.09	0.08
S28	-0.17	-0.17	-0.17	-0.17
H49	0.07	0.07	0.07	0.07
C30	0.07	0.07	0.07	0.07
H50	0.07	0.07	0.07	0.07
C31	0.08	0.08	0.08	0.08
H51	0.07	0.07	0.07	0.07
H52	0.07	0.07	0.07	0.07
C32	0.07	0.07	0.07	0.07
H53	0.07	0.07	0.07	0.07
H54	0.07	0.07	0.07	0.07

F. UV-visible spectra of N-PAA

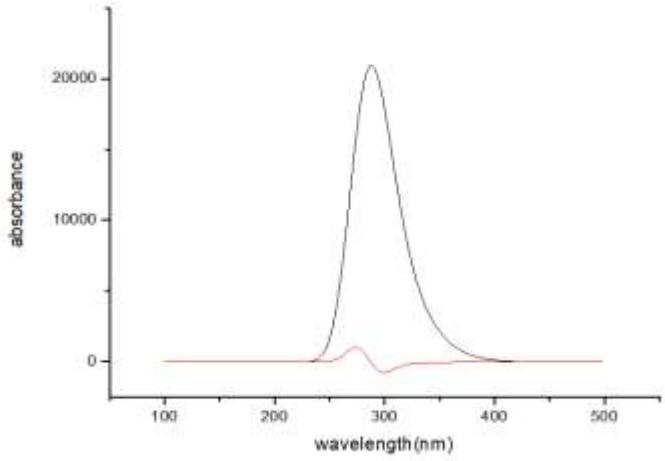

Fig. 4. *Spectra of N-PAA, an N-phenylacetamide derivative, in the UV and visible range*

Using GaussView 6 software, the UV-visible spectra of a complicated N-phenylacetamide derivative are examined in Fig. 4. The spectra revealed strong absorption of ultraviolet light, specifically a notable peak at 300 nm, representing the maximum absorption wavelength. This peak correlated with an absorbance value of 2000. The data was graphically presented, with wavelengths on the x-axis (0 to 500 nm) and absorbance on the y-axis (0 to 2000), showcasing the molecule's pronounced light absorption at 300 nm.

UV-visible spectra effectively elucidated the electronic transitions occurring in the intricate N-phenylacetamide derivative and absorption at 300 nm pointed to heightened UV light absorption due to the presence of conjugated systems or chromophores within the molecule. This detailed understanding of the compound's electrical and optical characteristics carried implications for potential applications across diverse industries, including photochemistry, sensors, and photovoltaics. The use of GaussView 6 software facilitated the acquisition and interpretation of UV-visible data, enriching the comprehension of the compound's spectral properties and contributing to a broader grasp of its attributes.

G. IR spectra of N-PAA derivative of N-phenylacetamide

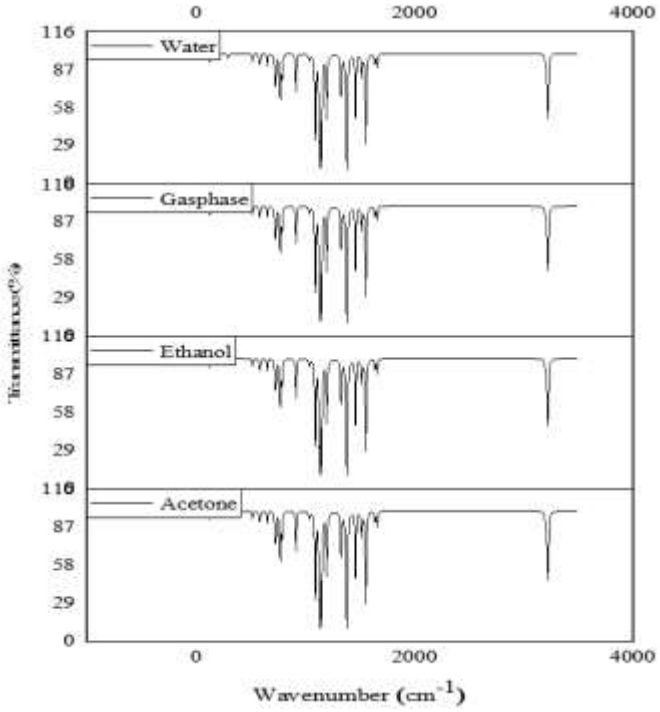

Fig. 5. *IR spectra of N-PAA derivative of N-phenylacetamide*

Examined the IR spectra of a complicated N-phenylacetamide derivative in various media, including ethanol, gas phase, acetone, and water. Data collection was made easier using the GaussView 6 program. Ten different peaks, with wavelengths ranging from 800 to 1800 cm^{-1}, were seen in the IR spectra and displayed a variety of vibrational modes and functional groups. Additionally, a prominent peak at approximately 3300 cm^{-1} denoted a crucial vibrational mode.

Analysis of the IR spectra allowed for the identification of the compound s functional groups. Each peak within the 800 to 1800 cm^{-1} range corresponded to specific functional groups with characteristic absorption frequencies. Accurate wavenumber values and peak intensities were documented from the observed IR spectra. These data were employed to create a scientific graph illustrating the compounds IR spectra. The graph displayed absorption peak intensity on the y-axis and wavenumber (cm^{-1}) on the x-axis (ranging from 800 to 1800 cm^{-1}). Peaks were labeled or color-coded to indicate the associated functional groups they

represented. An additional significant vibrational mode was evident around 3300 cm^{-1}.

IV CONCLUSION

This work used computational methods to investigate the structural and electrical characteristics of N-phenylacetamide derivatives (N-PAA and N-PAB), including Gaussian 09W and Gaussian 16 with B3LYP and M06-2X functionals. In order to evaluate different characteristics, including bond lengths, angles, dihedral angles, and Mulliken charge distributions, analysis was carried out at Riphah International University's chemistry department using UV and IR spectroscopic methods as well as DFT/B3LYP and MP2 methodologies. For reliable findings and an evaluation of the solvent impact, the DFT/B3LYP/6-31G(d) model was essential. Insights into shape, stability, and behaviour across solvents were provided by the results, which affected electronic structure, charge distribution, and reactivity. The work successfully combines computational approaches and spectroscopic methods to further our understanding of these substances and their applications in chemical analysis and material science.

ACKNOWLEDGEMENT

I would like to thank Riphah International University Faisalabad for supporting an environment that allowed for such creative research. Their commitment to expanding the frontiers of molecular science and their encouragement of multidisciplinary cooperation unquestionably contributed significantly to the accomplishment of this task.

Authors:

First Author – Muhammad Sikandar Subhani, Department of Chemistry, Riphah International University, Faisalabad,

Second Author – Namra Yaseen, M.phil Scholar Chemistry, Riphah International University, Faisalabad,

Third Author: Laiba Waris, M.phil Scholar Chemistry, Riphah International University, Faisalabad,

Fourth Author– Dr. Majid Ali, Assistant professor, Department of Chemistry, Riphah International University, Faisalabad

Fifth Author – Dr. Farhat Ibraheem, Riphah International University, Faisalabad,

Sixth Author – Dr. Mudasir Majeed, Research officer, Central Hi-Tech Lab, Government College University, Faisalabad,

Seventh Author – Namra, M.phil Scholar Chemistry, Riphah International University, Faisalabad,

Eighth Author – Dr. Fiaz Hussain, Assistant professor, Department of Fiber and Textile Technology, University of Agriculture Faisalabad,

Ninth Author – Muhammad Adnan, M.phil Scholar Chemistry, Riphah International University, Faisalabad,

Tenth Author – Dr. Azam Ali, Senior Research Scientist, Technical University of Liberec,

Correspondence Author – Dr. Majid Ali, Assistant professor, Department of Chemistry, Riphah International University, Faisalabad

REFERENCES

[1] J. Gonçales *et al.*, "Cannabis and its secondary metabolites: their use as therapeutic drugs, toxicological aspects, and analytical determination," *Medicines*, vol. 6, no. 1, p. 31, 2019.

[2] A. D. Dahlén *et al.*, "Trends in antidiabetic drug discovery: FDA approved drugs, new drugs in clinical trials and global sales," *Frontiers in Pharmacology*, vol. 12, p. 807548, 2022.

[3] A. Chand and H. S. Biswal, "Hydrogen bonds with chalcogens: looking beyond the second row of the periodic table," *Journal of the Indian Institute of Science*, vol. 100, pp. 77-100, 2020.

[4] V. Yele, M. A. Azam, and A. D. Wadhwani, "Synthesis, Molecular Docking and Biological Evaluation of 2-Aryloxy-N-Phenylacetamide and N′-(2-Aryloxyoxyacetyl) Benzohydrazide Derivatives as Potential Antibacterial Agents," *Chemistry & Biodiversity*, vol. 18, no. 4, p. e2000907, 2021.

[5] B. K. Das and D. Chakraborty, "Deciphering the competitive inhibition of dihydropteroate synthase by 8 marcaptoguanine analogs: Enhanced potency in phenylsulfonyl fragments," *Journal of Biomolecular Structure and Dynamics*, vol. 40, no. 23, pp. 13083-13102, 2022.

[6] M. G. Salem, Y. M. A. Aziz, M. Elewa, M. S. Nafie, H. A. Elshihawy, and M. M. Said, "Synthesis, molecular modeling, selective aldose reductase inhibition and hypoglycemic activity of novel meglitinides," *Bioorganic Chemistry*, vol. 111, p. 104909, 2021.

[7] R. Kakkar, "Isatin and its derivatives: a survey of recent syntheses, reactions, and applications," *MedChemComm*, vol. 10, no. 3, pp. 351-368, 2019.

[8] K. Srivani, T. Thirupathaiah, E. Laxminarayana, and M. Thirumala Chary, "An Efficient Synthesis of 2-(3-ARYL-1, 2, 4-OXADIAZOL-5-YL)-N-Phenylacetamide Derivatives," *Rasayan Journal of Chemistry*, vol. 11, no. 3, 2018.

[9] R. Karan, P. Agarwal, M. Sinha, and N. Mahato, "Recent advances on quinazoline derivatives: A potential bioactive scaffold in medicinal chemistry," *ChemEngineering*, vol. 5, no. 4, p. 73, 2021.

[10] Z. Rouifi *et al.*, "Synthesis, characterization and corrosion inhibition potential of newly benzimidazole derivatives: combining theoretical and experimental

study," *Surfaces and Interfaces*, vol. 18, p. 100442, 2020.

[11] E. R. Mohammed and G. F. Elmasry, "Development of newly synthesised quinazolinone-based CDK2 inhibitors with potent efficacy against melanoma," *Journal of Enzyme Inhibition and Medicinal Chemistry*, vol. 37, no. 1, pp. 686-700, 2022.

[12] A. Manhas, S. Kediya, and P. C. Jha, "Pharmacophore Modeling Approach in Drug Discovery Against the Tropical Infectious Disease Malaria," *Frontiers in Computational Chemistry: Volume 6*, vol. 6, pp. 132-192, 2022.

[13] P. V. Bharatam, "Computer-aided drug design," *Drug Discovery and Development: From Targets and Molecules to Medicines*, pp. 137-210, 2021.

[14] V. Yele, D. K. Sigalapalli, S. Jupudi, and A. A. Mohammed, "DFT calculation, molecular docking, and molecular dynamics simulation study on substituted phenylacetamide and benzohydrazide derivatives," *Journal of Molecular Modeling*, vol. 27, no. 12, p. 359, 2021.

[15] Y. Qiu, X. Li, X. He, J. Pu, J. Zhang, and S. Lu, "Computational methods-guided design of modulators targeting protein-protein interactions (PPIs)," *European Journal of Medicinal Chemistry*, vol. 207, p. 112764, 2020.

[16] S. Roy, A. Ukil, and P. K. Das, "Anti-infectives to Combat Leishmaniasis," *Frontiers in Clinical Drug Research: Anti-Infectives, Bentham Science Publishers, Singapore*, pp. 174-208, 2021.

[17] A. Verma, D. K. Waiker, B. Bhardwaj, P. Saraf, and S. K. Shrivastava, "The molecular mechanism, targets, and novel molecules in the treatment of Alzheimer's disease," *Bioorganic Chemistry*, vol. 119, p. 105562, 2022.

[18] R. E. Abdelwahab, A. F. Darweesh, M. A. Ragheb, I. A. Abdelhamid, and A. H. Elwahy, "Synthesis of New 2-(4-(1, 4-Dihydropyridin-4-yl) Phenoxy)-N-Arylacetamides and Their Heterocyclic-Fused Derivatives via Hantzsch-Like Reaction," *Polycyclic Aromatic Compounds*, vol. 43, no. 3, pp. 1974-1986, 2023.

[19] O. Fergachi *et al.*, "Experimental and Theoretical Study of Corrosion Inhibition of Mild Steel in 1.0 M HCl Medium by 2 (-4 (hloro phenyl-1H-benzo [d] imidazol)-1-yl) phenyl) methanone," *Materials Research*, vol. 21, 2018.

[20] A. D. Pagar, M. D. Patil, D. T. Flood, T. H. Yoo, P. E. Dawson, and H. Yun, "Recent advances in biocatalysis with chemical modification and expanded amino acid alphabet," *Chemical Reviews*, vol. 121, no. 10, pp. 6173-6245, 2021.

[21] Y. Lee, S. Basith, and S. Choi, "Recent advances in structure-based drug design targeting class AG protein-coupled receptors utilizing crystal structures and computational simulations," *Journal of Medicinal Chemistry*, vol. 61, no. 1, pp. 1-46, 2018.